



departement
Mobiliteit en
Openbare Werken

Experimental investigation on consolidation behavior of mud

Subreport 1:
METHODOLOGY STUDY



12_082

WL Rapporten

Experimental investigation on consolidation behaviour of mud

Subreport 1- Methodology study

Meshkati Shahmirzadi, M. E.; Staelens, P.; Claeys, S.; Cattrysse, H., Van Hoestenbergh, T.; Van Oyen, T.;
Vanlede, J.; Verwaest, T.; Mostaert, F.

June 2015

WL2015R12_082_1

This publication must be cited as follows:

Meshkati Shahmirzadi, M. E.; Staelens, P.; Claeys, S.; Cattrysse, H., Van Hoestenbergh, T.; Van Oyen, T.; Vanlede, J.; Verwaest, T.; Mostaert, F. (2015). Experimental investigation on consolidation behaviour of mud: Subreport 1- Methodology study. Version 5.0. Pick an item, 12_082. Flanders Hydraulics Research: Antwerp, Belgium.



Waterbouwkundig Laboratorium

Flanders Hydraulics Research

Berchemlei 115

B-2140 Antwerp

Tel. +32 (0)3 224 60 35

Fax +32 (0)3 224 60 36

E-mail: waterbouwkundiglabo@vlaanderen.be

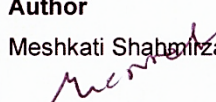
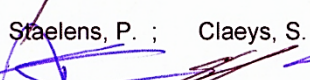
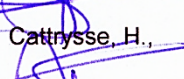
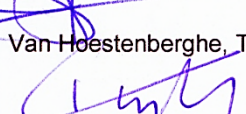




www.waterbouwkundiglaboratorium.be

Nothing from this publication may be duplicated and/or published by means of print, photocopy, microfilm or otherwise, without the written consent of the publisher.

Document identification

Title:	Experimental investigation on consolidation behaviour of mud: Subreport 1- Methodology study		
Customer:	aMT	Ref.:	WL2015R12_082_1
Keywords (3-5):	mud, consolidation		
Text (p.):	26	Appendices (p.):	/
Confidentiality:	<input type="checkbox"/> Yes	Exceptions:	<input type="checkbox"/> Customer
	<input checked="" type="checkbox"/> No		<input type="checkbox"/> Internal
			<input type="checkbox"/> Flemish government
		Released as from: /	
		<input checked="" type="checkbox"/> Available online	

Approval

Author	Reviser	Project Leader	Research & Consulting Manager	Head of Division
Meshkati Shahmirzadi, M. E.  Staelens, P. ; Claey s, S.  Catrysse, H.,  Van Hoestenbergh e, T. 	Vanlede, J. 	Van Oyen, T. 	Verwaest, T. 	Mostaert, F. 

Revisions

Nr.	Date	Definition	Author(s)
1.0	06/08/2013	Concept version	Meshkati Shahmirzadi, M. E.; Staelens, P. Catrysse, H.; Claey s, S., Van Hoestenbergh e, T.,
2.0	28/08/2014	Substantive revision	Vanlede, J.
3.0	08/12/2014	Revision customer	Chantal Martens
4.0	20/05/2015	Revision customer	Chantal Martens
5.0	02/06/2015	Final version	Van Oyen, T., Meshkati Shahmirzadi, M.E.

Abstract

Due to the complex nature of mud consolidation within harbours, a robust and accurate guideline to evaluate the nautical depth is still under debate. Besides, alternative dredging techniques (e.g. mud conditioning/fluidising) have proven to be an applicable method to reduce dredging costs in a number of harbours. Yet, before one can define new criteria for nautical depth or implement new dredging techniques, a deeper understanding of the temporal evolution of rheological, mechanical and biological characteristics of mud is needed. In this study, we aim to improve the understanding of the rheological properties of consolidating mud by comparing the consolidation process of mud from 5 different locations namely the harbours of Zeebrugge (ZB) and Deurganckdok (DG) in Belgium, the harbours of Rotterdam (RO) and IJmuiden (IJ) in the Netherlands and the Emden (EM) harbour in Germany. The main objectives of this project are to examine the effect of the consolidation process on the mechanical, rheological and biological characteristics of mud as well as to explain the differences in consolidation processes between muds from different origins.

This sub-report describes the properties of different mud types used for the experiments as well as the experimental setup. The experimental setup includes a detailed description of the governing parameters, experimental design and measurement techniques conducted on two different consolidation columns, small and large.

Contents

1. Introduction.....	1
2. Experimental set-up.....	3
2.1. Mud types.....	3
2.2. Setup of small consolidation columns	4
2.3. Setup of large consolidation columns	4
3. Measurements.....	7
3.1. Small consolidation column (SC)	7
3.1.1. Measurement Frequency	7
3.1.2. Rheology	9
3.1.3. Density	14
3.1.3. Grain size	16
3.1.4. Dry matter, organic and carbonate content.....	17
3.2. Large consolidation column (LC)	17
3.2.1. Measurement Frequency	18
3.2.2. Image Processing	19
3.2.3. Pore water pressure and effective stress.....	23
4. References	24
5. Appendix.....	26

List of tables

Table 1 - the summary of planned sub-reports for the entire research project.....	2
Table 2 - Properties of the different muds used in this study (Merkelbach, 1999).	3
Table 3 - Dates and measurements types conducted on SCs;	8
Table 4 - The sampling characteristics of Rheometer test developed for characterizing the rheological properties.....	12
Table 5 - Dates and measurements conducted on LCs.	18

List of figures

Figure 1 - The origins of the five mud samples studied in this research project.....	3
Figure 2 - Set of small consolidation columns for different harbors (SCs).	4
Figure 3 - a) The large consolidation columns (LCs) with riser tubes; b) The ball valves connecting the riser tubes to the LCs.	5
Figure 4 - a) Sampling form the SC using Beeker sampler; b) Piston.....	6
Figure 5 - The Anton Paar MCR 301 Rheometer of the Flanders Hydraulic Laboratory with the vane used in this research.	9
Figure 6 - The variation of shear stress versus time for a rotation rate of 1 rpm for Zeebrugge mud with a 1.2 g/cm ³ density.....	11
Figure 7 - A typical shear stress-time relationship obtained by execution of the full test sequence of the long protocol for Zeebrugge mud with a 1.2 g/cm ³ density.	11
Figure 8 - Method for selecting the appropriate protocol for each sub-sample of a SC.	13
Figure 9 - EF-curve (EFC) derived with the long protocol as shown in Figure 7. The Y-axis shows shear stress as estimated from the rheometer from the measured Torque.....	14
Figure 10 - The Anton Paar DMA 38 density meter used in FHR laboratory.....	15
Figure 11 - The Radioactive densitoscanner and the installation setup for SCs	16
Figure 12 - Mastersizer 2000 from the laboratory of FHR.	16
Figure 13 - Prepash device from the laboratory of FHR to derive dry matter, organic matter and carbonate content.	17
Figure 14 - The camera setup monitoring the evolution of mud consolidation within five LCs.....	19
Figure 15 - Illustration of an image of one of the camera's with location of the yellow balls showing the pore water pressures for different riser tubes (red circle) and the mud interface (blue circle) in a LC.	20
Figure 16 - Detecting the decimeter markings on yellow rulers.....	20
Figure 17 - The 3rd degree polynomial fit between the decimeter points on the rulers.....	21
Figure 18 - A typical pixel-to-distance map.	21
Figure 19 - Time series of the position of the ball in the riser tube of Zeebrugge LC over time by calculating the yellow spectrum of all pixels in a column.....	22
Figure 20 - Time series of the complete spectrum depicting the mud interface within one LC.	22
Figure 21 - The position of the ball in actual distance over time for one LC.....	22
Figure 22 - The position of the mud interface in actual distance over time for Zeebrugge harbour.	23

1. Introduction

Harbours and ports are of vital importance to the world's economy since they provide a link between land and sea transportation. Due to the continuously increasing worldwide demand for raw materials, ships are expanding in size. In this respect, the bigger the ship, the larger the economic benefits will be. Unfortunately, the size of harbours is often restricted by natural constraints. In many harbours a significant limit is posed by the continuous import of (cohesive) sediment into the harbour which confines the navigability and inflicts high dredging costs.

The nautical bottom/depth determination is defined by PIANC (1997) as: "The level where the physical characteristics of the bottom reach a critical limit beyond which contact with a ship's keel causes either damage or unacceptable effects on controllability and manoeuvrability". Unfortunately, due to the consolidation process, the characteristics of the mud layer vary spatially and in the vertical direction (towards the bottom). For instance, the density of the fluid-mud mixture changes with depth as well as its rheological properties. As such, the in-situ accurate determination of the local nautical depth, at which the rigidity of the mud will cause severe navigational problems, is not straightforward. In fact, due to the highly complex nature of mud consolidation within harbours, an accurate and robust general guideline for finding the nautical depth is still under debate.

Presently, mud density is considered as overall indicator to reflect the nautical bottom in Zeebrugge (Delefortrie et al., 2005). Historically, the critical cohesive sediment density level was linked to an in-situ density level of 1.15 g/cm³ (Kerckaert et al, 1985; 1988; Van Craenenbroeck and Vantorre, 1991 and 1992). Later on, a critical density of 1.2 g/cm³ was adopted, based on an extensive experimental and modelling investigation of ship manoeuvrability (Delefortrie et al., 2005). In addition, in case the imported sediment mainly consists of fine material (grain size < 60 μ m), the sedimentation of the cohesive sediment leads to muddy layers above the nautical depth with different characteristics. Presently, in Zeebrugge the maximum level of this "black water" is defined by considering that maximum 7% of the ship's keel may be submerged into this muddy layer.

Although very costly, port authorities nowadays dredge high volumes of mud every year to guarantee a safe and quick navigation. In this regard, as indicated above, the criteria commonly used to determine until which depth should be dredged is density. However, because of the complex composition of consolidating mud, it is possible that different mixtures react differently to deformation while having the same density. Hence, it is obvious that a parameter which is directly related to the sediment rheology and strength of the mud layer could be a more efficient criteria to determine dredging needs instead of density (Guiarte et al., 1979).

Alternative dredging techniques (e.g. mud conditioning/fluidising) have proven to be an applicable method to significantly reduce the dredging costs in a number of harbours, e.g. Emden or Ijmuiden (Wurpts and Torn, 2005). Yet, before one can define new criteria for nautical depth or implement new dredging techniques, a deeper understanding of the temporal evolution of rheological properties of mud and its interdependence with other factors such as mechanical and biological characteristics of mud.

The overall goal of this study is to enhance our understanding of the rheological properties of consolidating mud by comparing the consolidation process of mud from 5 different locations. In particular, we seek to answer why rheological properties (e.g. strength) of mud from different origins differ. We anticipate that by answering this question provides additional insight for a more realistic definition of the nautical bottom. Moreover, exploring the secret behind the different behaviour of different mud types may provide us the capability to control the rate of consolidation, and the strength of mud within the harbours.

The research project on the consolidation behaviour of mud aims to address the following objectives:

- examine the effect of the consolidation process on the mechanical, rheological and biological characteristics of mud.
- explain the differences in consolidation processes between muds from different origins.
- investigate the correlation between different governing parameters e.g. peak shear stress (rheological) and organic matter content (biological).
- furnish the foundation for practical recommendations and design guidelines for mud treatment
- highlight the current issues and future challenges faced for conducting experiments on consolidation of mud.

The governing parameters that are taken into account in this study are the rheological characteristics (e.g. peak shear stress, equilibrium flow curves), some mechanical characteristics (e.g. density, grain size composition, pore water pressure, effective stress) and some biological characteristics (e.g. carbon and organic content) of mud. To measure these parameters a series of systematic and parallel experiments were designed. These experiments were initiated on the 4th of May 2014 and continued till the 20th of August 2014.

Here, it is worth to note that the execution of the consolidation experiments described in this sub-report is based on a related method statement. This method statement was distilled out of a throughout brainstorming on consolidation processes, feasibility study, design of the set-up and planning of the factual execution where through a comprehensive method statement the most important mineralogical, biological and chemical parameters is described (Claeys et al., 2015a).

The current sub-report is divided into 2 main chapters summarized as follows:

- chapter 2 describes the properties of different mud types used for the experiments as well as the experimental setup.
- chapter 3 includes a detailed description of the experimental design and measurement techniques. In this chapter the measurements conducted on two different consolidation columns, small and large, are distinguished.

Therefore, the current sub-report is only devoted to a comprehensive description on the model setup and experimental procedures. The experimental results will be presented in a different manuscript, called subreport 2, which is currently in preparation. Finally, the first and second sub-report will be followed by a third sub-report which analyses the obtained results in depth and answers the main research questions mentioned in the introduction. Table 1 provides the summary of planned sub-reports for the entire research project.

Table 1 - the summary of planned sub-reports for the entire research project.

Sub-report NO.	Sub-title	Delivery Status
1	Methodology report	Current manuscript
2	Factual data report	In preparation
3	Results and discussion report	In preparation

2. Experimental set-up

In this chapter, general information about the experimental set-up is provided. Besides, the motivation for the mud types from the different harbours, as well as the general set-up of the experiments in small and large columns are described.

2.1. Mud types

We analysed mud from five different origins, namely the harbours of Zeebrugge (ZB) and Deurganckdok (DG) in Belgium, the harbours of Rotterdam (RO) and Ijmuiden (IJ) in the Netherlands and the Emden (EM) harbour in Germany. These five locations cover a shore area along the Ems estuary, the Rhine-Meuse estuary and the Scheldt estuary as shown in Figure 1.

Comparing the consolidation behaviour of mud from different locations increases the variation in the data sets by taking into account a distribution of the key parameters such as different harbour configurations, salinity conditions, geological characteristics of mud and governing flow and tidal conditions in the vicinity of the harbour. This might broaden the practical use of the results. Table 2 presents an overview on some general properties of mud types from Emden and Rotterdam. Unfortunately, no such data are available for other harbours. These properties will be determined for the other harbours and will be presented in sub-report 3.

Table 2 - Properties of the different muds used in this study (Merkelbach, 1999).

Mud Types	Density of solids (g/cm ³)	Sodium adsorption ratio (-)	Cation exchange capacity (cmol/kg)	specific surface (m ² /g)	Humus (% by weight)
Rotterdam	2.5278	70	20.1	96	3.99
Emden	2.6362	42	18.0	108.23	3.05

For every harbour, mud was sampled (1 till 2 m³) in bulk. These dredged volumes were transported in bulk containers to the Flanders Hydraulics Laboratory where they were diluted with water from their corresponding origin and treated to the desired initial condition as explained in Section 2.4 and Page 5.



Figure 1 - The origins of the five mud samples studied in this research project (figure adopted from Google Earth).

2.2. Setup of small consolidation columns

A number of small consolidation columns are adopted to monitor the consolidation behaviour of mud from its initial condition through the different consolidation phases. For the sake of brevity, the small consolidation column is called SC hereafter in this manuscript. The goal is to obtain undisturbed samples of mud for different stages of the consolidation process. In this respect, for each mud type 6 small consolidation columns (57 mm inner diameter) are filled with mud with the same starting condition. The type and diameter of the SCs are the same as a Beaker sampler to facilitate the sub-sampling process. The sub-sampling process is described in section 2.5. In total for the 5 harbours 30 consolidation columns are installed. The height of a small consolidation column is 3 m. Figure 2 depicts the SC sets.



Figure 2 - Set of small consolidation columns for different harbors (SCs).

2.3. Setup of large consolidation columns

In addition to 6 SCs for each location, one large consolidation column (LC) with an inner diameter of 160 mm is used for each mud type. Experiments in the past have shown that processes in laboratory columns, particularly settling and consolidation, can be influenced by the diameter of the columns. In general, the smaller the diameter of a column is, the slower the rate of consolidation (Migniot, 1987; Huysentruyt and Berlamont, 1993). Michaels and Bolger (1962), however, showed that the study of flocculated suspensions of kaolin could be carried out in columns of 48 mm diameter without fear of wall friction. Van Goethem et al. (1985) found no difference in the relative residual height between columns with 0.1 m diameter and those with 1 m diameter. Miegheem et al. (1997) also recommended a minimal diameter of 0.1 m for consolidation experiments, while U. S. Army Corps of Engineers (1987) suggested a column with 2.032 m (8-inch) diameter to be constructed for consolidation/dewatering tests. Hence, we anticipate that due to wall effects the data obtained using small-diameter columns will not accurately reflect field consolidation behaviour. In the literature, a consolidation column with an inner diameter smaller than 100 mm is referred to as small (Johansen, 1998; Lintern, 2003; Merckelbach, 1998). Consideration of the robustness of the column, the ease of manipulation, the use of glues to mount the riser tubes and the transparency, the LCs in this project have been designed for 16 cm width. A width of 16 cm also brings the possibility of profiling with a Beaker sampler in the LC at the end of an experimental period.

The consolidation of the mud within the LC of each location was monitored for a period of four months starting from the beginning of the experiments 7th of April till the 20th of August 2014. In particular, the time-dependent variation of the mud interface as well as the pore water pressure variation along the depth axis of the column is monitored. To measure the pore water pressure distribution, a ball valve was

connected every 20 cm along the depth axis of the LCs to connect the riser tubes with the mud through a filter with a diameter of 2 cm. The first riser tube was connected to the LCs at a level of 12.5 cm height from the ground. Figure 3 shows the large consolidation columns equipped with riser tubes. Both small and large consolidation columns were sealed on top and bottom to prevent the evaporation and leakage of mud and water from the column, respectively. The consolidation columns were installed on a multiplex wall anchored with metal bars to keep the consolidation columns vertically stable.

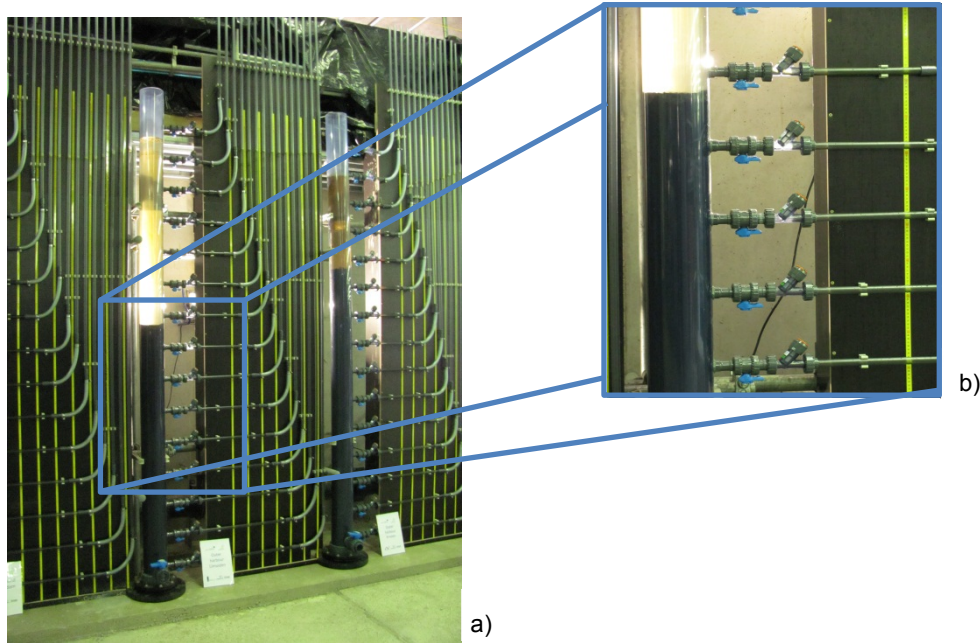


Figure 3 - a) The large consolidation columns (LCs) with riser tubes;
b) The ball valves connecting the riser tubes to the LCs.

2.4. Initial conditions

The mud from the different harbours was diluted to a set density of 1.1 g/cm^3 . Each mud was diluted with water from its corresponding origin to increase the resemblance of the consolidation process with the in-situ conditions. In case of Emden, water from River Scheldt with similar salinity was used for dilution due to a lack of native water. The homogeneous mixture was poured into the consolidation columns until a height of 2.75 m was reached. The desired initial condition (density= 1.1 g/cm^3) is obtained through conducting the following steps:

- a) Mixing the mud within an IBC (bulk container)
- b) Examining the density of mud within the IBC and adding or removing water from IBC in case the density differs from the desired density (1.1 g/cm^3).
- c) When the desired density of mud is obtained, using buckets mud will be brought to the top of the LC. Thereafter, mud will be poured into the LC using a funnel and a tube.

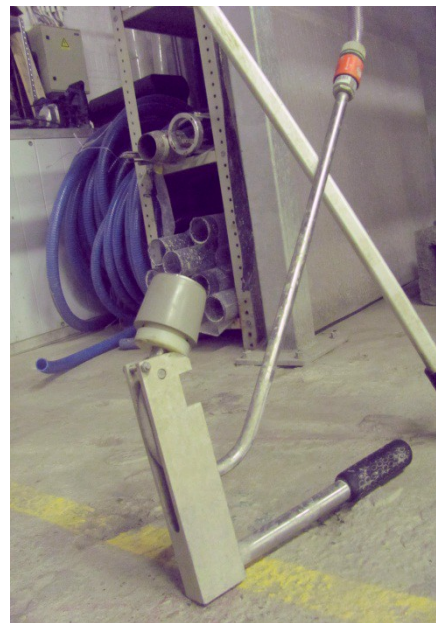
A value of 1.1 g/cm^3 is chosen as initial density since it provides a condition close to the gelling point for the mud-water mixture within the consolidation column. The transition between sedimentation and consolidation is characterised by the gel point (Buscall, 1990). The gelling point is the critical volumetric concentration at which soil formation starts. For North-Sea mud, the gel point is found to be about 1.1 g/cm^3 for soil bulk densities. This explains the apparent fluid-like behaviour of freshly deposited mud (with a density of about 1.1 g/cm^3), since its structure is easily disturbed (Lee et. al., 2012).

2.5. Sampling method

To sample the mud from the SCs, the Beaker sampling method is used. With this method, the mud within SC is slowly pushed upwards along the tube and the samples are taken at the upper part of the SC. Using a tripod, the SC is kept vertically and connected to a piston at its bottom end. This piston provides the required water head to push up the mud. The speed of sampling can be adjusted by the opening ratio of the valve that connects the piston to tap water. A 10 cm high subsample is then located at the top of the SC. Opening the valve pushes the mud upwards into the Beaker sampler. When the 10 cm sub-sampler is filled up with mud, the valve is closed and a metal device (sample divider) is used to separate the subsample from the SC. The participating system and piston is shown in Figure 4a and b. The sub-sampled mud is then immediately delivered to the laboratory for analysis. A description on the the Beaker sampling method is provided in Eijkelkamp (2005). The samples were numbered from top (first sample) till bottom.



a)



b)

Figure 4 - a) Sampling form the SC using Beaker sampler; b) Piston.

3. Measurements

This section aims to provide a detailed description of the measurement techniques that were applied in this project. The measurement techniques and the execution dates of experiments conducted on the sub-samples from the small consolidation columns (SCs) differ from those of the large consolidation columns (LCs). Hence, the description is provided in two separate subsections. All the measurements were conducted at Flanders Hydraulics Research (FHR) that has ISO-accreditation for all the analyses mentioned in this section.

3.1. Small consolidation column (SC)

To obtain insight in the time dependent consolidation behaviour of the different muds, 5 out of 6 SCs were sub-sampled (consumed) at different time points, namely 1, 7, 14, 28 and 56 days after initiation of the experiments. As described in chapter 2, the SCs are sub-sampled using the Beeker sampler method and subsequently analysed in the laboratory. The last SC (the 6th) of each mud type, however, was kept to measure the vertical density distribution on the same time points, using a Radioactive densitoscanner. The last SC of each mud type is sub-sampled at the end of the experimental period, i.e. 135 days after the initiation of experiments. The choice of time intervals for consumption of the small consolidation columns and scanning of the densities is based on research executed by Flanders Hydraulic Research (Claeys, et al., 2009; Wurpts and Greiser, 2008).

3.1.1. Measurement Frequency

Table 3 provides an overview of all measurements conducted on the sub-samples from the small consolidation columns. For each measurement the corresponding execution date is presented. In this table, each measurement type is coded by a colour. The number within a coloured cell corresponds to the number of the small consolidation column. For instance, 4 refers to the 4th small consolidation column of each mud type, which were consumed at time point 4 (28 days after initiation). As can be seen in Table 3, the different measurements for a time point was conducted as soon as possible after sampling. An exception, however, was made for the grain size measurements. These were generally performed with a time delay of between 2 till 10 days, assuming that time would not affect significantly the grain size values.

Table 3 - Dates and measurements types conducted on SCs;
 the numbers refer to the time points (1= 1 day; 2= 1 week; 3= 2 weeks; 4=3 weeks; 5= 4 weeks; 6= 6 weeks).
 The colours refer to the type of manipulation or analyses.

Date	07/4	08/4	09/4	10/4	11/4	14/4	15/4	16/4	17/4	18/4	21/4	22/4	23/4	24/4	28/4	29/4	05/5	06/5	07/5	15/5	16/5	02/6	03/6	04/6	05/6	09/6	11/6	12/6	22/8	25/8	05/8	17/8	18/8		
ZB	Filling	Rheological 1				DMA 2 2	PrepAsh 1 2	Grain Size 2					DMA 3 3 3				Radioactive 4 4 4	PrepAsh 4		Grain Size 3 4		DMA 5 5	Radioactive 5			Grain Size 5			DMA 6 6 6	PrepAsh 6					
DG		Filling	Rheological 1			DMA 2 2	PrepAsh 1 2	Grain Size 2					DMA 3 3 3				Radioactive 4 4 4	PrepAsh 4		Grain Size 3 4		DMA 5 5	Radioactive 5			Grain Size 5			DMA 6 6 6	PrepAsh 6					
RO			Filling	Rheological 1		DMA 1	PrepAsh 1	Grain Size 1					DMA 2 2 2	PrepAsh 2			Radioactive 3 3 3	PrepAsh 3		Grain Size 4 4		DMA 5 5	Radioactive 5			Grain Size 5			DMA 6 6 6	PrepAsh 6					
IJ			Filling	Rheological 1		DMA 1	PrepAsh 1	Grain Size 1					DMA 2 2 2	PrepAsh 2			Radioactive 3 3 3	PrepAsh 3		Grain Size 4 4		DMA 5 5	Radioactive 5			Grain Size 5			DMA 6 6 6	PrepAsh 6					
EM				Filling	Rheological 1	DMA 1 1	PrepAsh 1	Grain Size 1					DMA 2 2 2	PrepAsh 2			Radioactive 3 3 3	PrepAsh 3		Grain Size 4 4		DMA 5 5	Radioactive 5			Grain Size 5			DMA 6 6 6	PrepAsh 6					

Legend:

<p> Filling the SCs</p> <p> Rheological parameters</p> <p> DMA 38</p>	<p> Radioactive densitoscanner</p> <p> PrepAsh</p> <p> Grain Size</p>
--	--

3.1.2. Rheology

Measurement protocol

The strength characteristics of the mud types are of particular interest in this study. Therefore, the sub-sampled mud from SCs are analysed with the Rheometer from the laboratory of Flanders Hydraulic Research to obtain rheograms for each mud sub-sample. The measurement are conducted with an Anton Paar MCR 301 Rheometer, equipped with a vane ST22-4V-40 with diameter 21.9 mm and height 40.3 mm (Figure 5). For introducing a strain in the mud, a vane instead of a concentric-cylinder was used. This significantly reduces the structural changes of mud sample while testing (Merckelbach,1998). In the vane test, the rotational speed of the vane is translated to a shear rate and the torque is converted to shear stress.

A combined protocol was designed to measure the dynamic behaviour of mud upon exposure to different external forces under a shear-rate controlled test. This enables the results to be compatible with most of the executed international research on this topic (Toorman, 1997; Fontein and Wal, 2006). The use of this protocol assumes that all samples are composed of cohesive sediments. This means that they need to be tested as non-Newtonian like substances to cover all possible states.

More information on the protocol can be found in Claeys et al. (2015b, in preparation). The determination of the main rheological parameters will be explained in the following section.



Figure 5 - The Anton Paar MCR 301 Rheometer of the Flanders Hydraulic Laboratory with the vane used in this research.

Rheological parameters

- Peak shear stress

A Beaker sampler filled with an undisturbed sample was placed on the mounting platform of the Rheometer and the vane was lowered until fully submerged. Subsequently, a rotational speed of 1 rpm was applied for 60 seconds and the required shear stress was recorded in time (50 samples/second). Through this (first) phase of protocol the maximum resistance of the mud is obtained in the elastic phase before it shears (plastic behaviour). This maximum resistance is known as the peak shear stress and can be interpreted as the first resistance that a vessel experiences when it navigates through the mud. Moreover, it may reveal information on the consolidation status of the mud. Figure 6 depicts a typical shear stress-time relationship obtained through execution of the first phase of protocol. The peak shear stress given on this figure corresponds to the highest resistance of a diluted mud sample from Zeebrugge with a density of 1.2 g/cm^3 while being exposed to a 1 rpm rotation rate.

- Equilibrium shear stress and equilibrium flow curves (EFC tests)

A cycle in the protocol consists of an EFC-test just after pre-shearing the mud (before the mud structure is regained). The first EFC-test in the protocol introduces a deformation rate of 112 rpm for 100 seconds after the mud is presheared. The stress needed to maintain this deformation rate is recorded in time. The next cycle applies again a constant deformation rate until equilibrium after preshearing. These recordings depict the trajectory of the mud viscosity during shearing at different speeds which gives information about shear thinning processes of the mud during contact with different parts of the vessel (hull, rudder, and propeller) at different speeds (sailing speed, manoeuvring speed, and propeller rotation). By recording the dynamic mud viscosity, the model parameters (e.g. Worrall Tuliani) can be obtained to describe the EFC. The blue lines in Figure 7 indicates the EFC tests.

The Dullaert method is applied after each EFC-test to obtain the structural parameters of mud. Dullaert method records the retained stress of mud after applying the constant rotation speed in time (see Figure 7). Directly after an equilibrium is obtained in EFC-test, the Dullaert test is applied. During this test a very low rotation speed of 0.001 rev/sec is applied for 6 seconds and the corresponding shear stress is recorded (Claeys et al. 2015b; in preparation). Plotting the decreasing shear stress versus time can be used for the calculation of the thixotropic parameters.

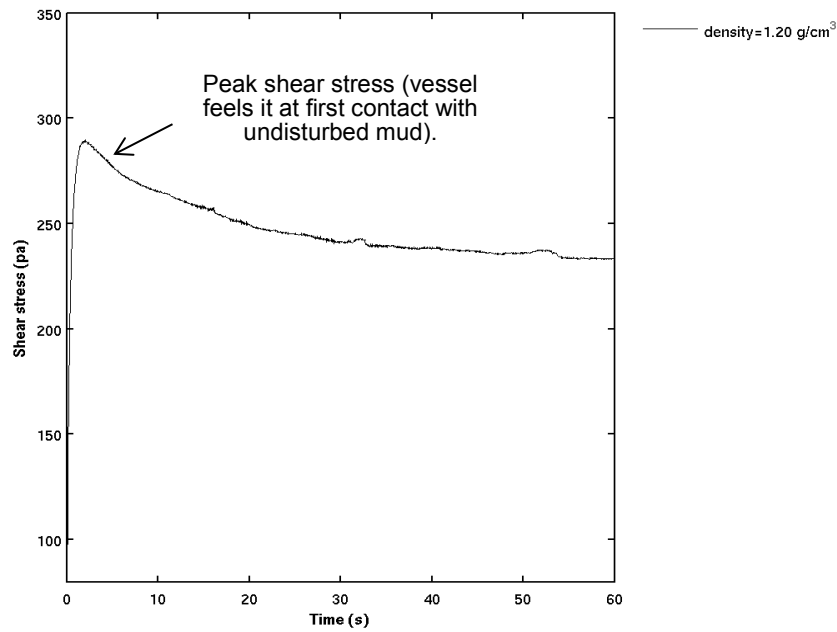


Figure 6 - The variation of shear stress versus time for a rotation rate of 1 rpm for Zeebrugge mud with a 1.2 g/cm³ density

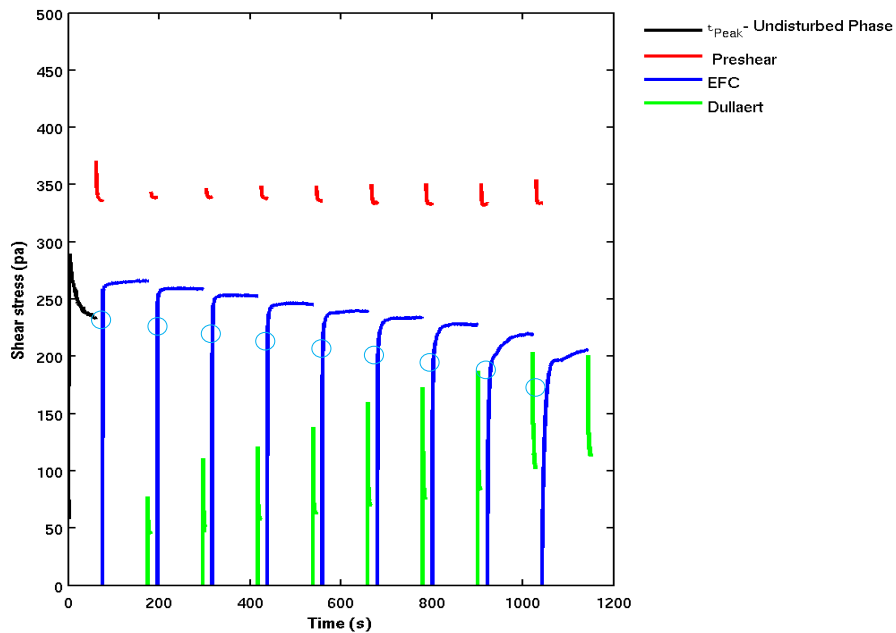


Figure 7 - A typical shear stress-time relationship obtained by execution of the full test sequence of the long protocol for Zeebrugge mud with a 1.2 g/cm³ density.
 The EFC-part consists of 9 cycles (9 different deformation rates) of preshearing followed by applying a constant rotation until equilibrium. The Y-axis shows instrument shear stress as estimated from the rheometer by considering the measured torque

An internal study in Flanders Hydraulic Research was conducted (Claeys et al., 2015b) to find the best applicable deformation rates and duration resulted in two procedures for EFC tests, namely a long and short protocol. In the long protocol, 9 EFC cycles were applied to the mud with rotation rates gradually decreasing from 112 to 56, 28, 14, 7, 4, 2, 0.5 and 0.2 rpm. The long protocol was applied to sample 1, 5, 9, 13, ... taken from the SCs. Execution of the long protocol on a sub-sample takes about 20 minutes. In the short the sub-sampled mud is exposed to only the 3 deformation rates of 112, 56 and 28 rpm to save time. The majority of the sub-sampled mud from SCs were examined with the short protocol procedure. The duration of EFC tests were the same for both long and short protocol, each EFC test measures the strength of mud over 100 seconds. Table 4 summarizes the sampling characteristics used for describing the rheological properties.

Table 4 - The sampling characteristics of Rheometer test developed for characterizing the rheological properties.

Rheometer set-up	Peak shear stress	Pre-shearing	EFC equilibrium points
Applied deformation rate (RPM)	1	1000	112*, 56*, 28*, 14, 7, 4, 2, 0.5, 0.2
Sampling time (sec)	60	15	100
Sampling rate (Hz)	50	1	2

*In case of short protocol, only three deformation rates of 112, 56 and 28 rpm were applied to the sub-samples.

Figure 8 explains the procedure which protocol to use for each sub-sample of the SCs. Assuming a SC is profiled into 24 sub-samples using the Beeker sampler method in which the sub-samples are numbered beginning with the number 1 at the top and continued until the last sub-sample number 24 at the bottom. The first of every four sub-samples is analysed with long protocol (numbers highlighted in red in Figure 8). On the other sub-samples the short protocol is applied (numbers highlighted in black in Figure 8).

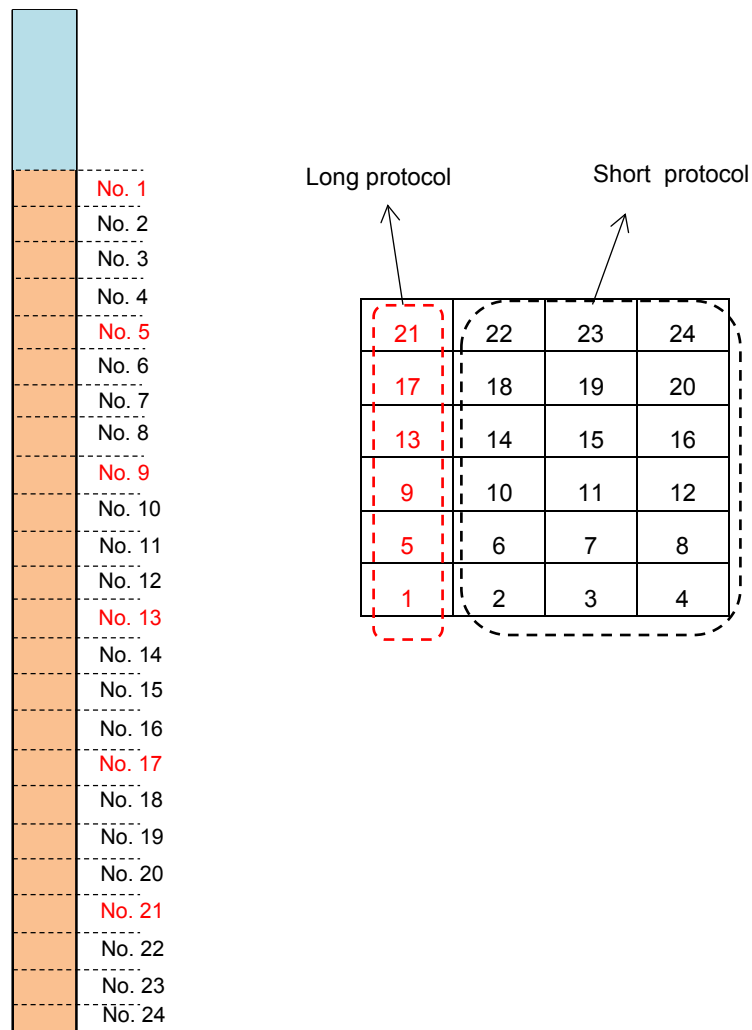


Figure 8 - Method for selecting the appropriate protocol for each sub-sample of a SC.

EFC tests provide equilibrium shear stresses for a given density and a given rotation rate. These equilibrium shear stresses are obtained once an asymptotic value is reached in the shear stress-time curve. These values are highlighted by a blue circle in Figure 7. The equilibrium flow curves (EFCs) can be obtained by plotting the equilibrium shear stress values against the corresponding rotation rates. A typical EFC for Zeebrugge mud with 1.2 g/cm³ density is shown in Figure 9. From these EFC curves a rheological model can be fitted.

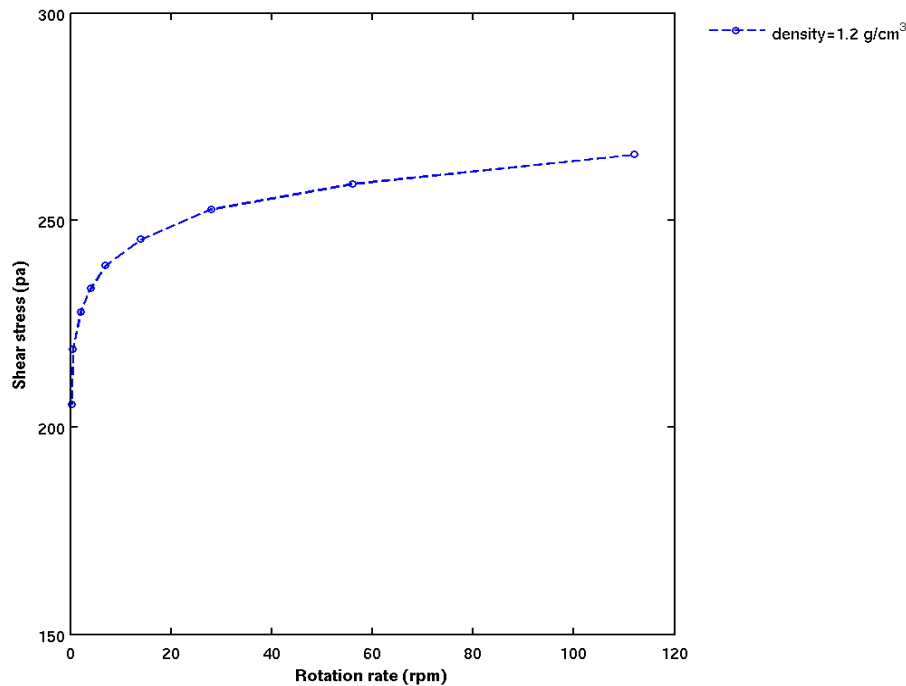


Figure 9 - EF-curve (EFC) derived with the long protocol as shown in Figure 7. The Y-axis shows shear stress as estimated from the rheometer from the measured Torque.

3.1.3. Density

The harbour of Zeebrugge uses bulk density as a criterion to follow up the Nautical Depth, but there are harbours where strength parameters are used (Wurpts, 2005). Measuring the strength of mud in situ, however, is a challenging task and not yet solved in the literature (Huang and Huhe, 2009). This is why researchers attempt to explore a relationship between strength of mud and a more tangible physical parameter such as density. In this regard, some authors claim that there is not a strong positive association between density and strength of mud (Staelens et al., 2013, Fontein and Wal, 2006), while others report such a relationship (e.g. Kerckaert et al., 1985).

DMA 38

The Anton Paar DMA 38 from Flanders Hydraulics Research is used to measure the density of each sub-sample from the SCs. The density measurements were repeated 2 times to achieve a higher accuracy. The DMA 38 measures densities of materials ranging between 0 till 3 g/cm³ ± 0.001 g/cm³ (manufacturer specifications). Before introducing the mud into the device with a syringe, the gas bubbles were released by subtly shaking the syringe. It should be taken into account that high density sludge is very difficult to pump up into the small vibrating (oscillation) tube, and obstruction can occur in case of large debris. The DMA 38 is shown in Figure 10.

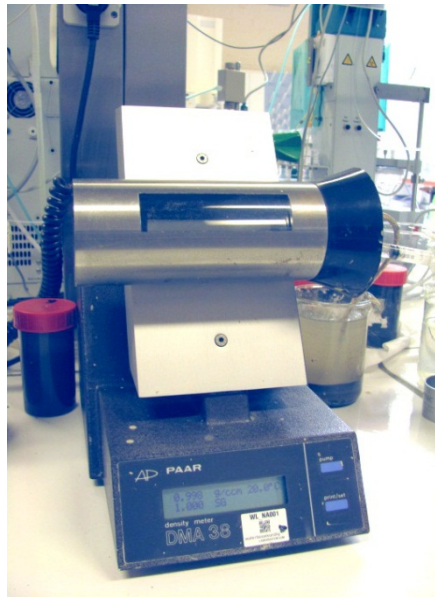


Figure 10 - The Anton Paar DMA 38 density meter used in FHR laboratory.

Radioactive densitoscanner

Disturbance of the sub-samples while using Anton Paar DMA 38, even though the syringe samples are taken with care is unavoidable. Thus, the Gamma ray density scanner is used to measure the vertical density of the last SC of each mud type. The purpose of this measurement is to map the density distribution along the depth axis without disturbing the mud.

As mentioned earlier, 5 out of 6 SCs are sub-sampled (consumed) for analysis in the laboratory approximately after 1 day, 1 week, 2 weeks, 4 weeks and 8 weeks. The 6th SC of each mud type, unsampled SCs, is kept to measure the vertical density distribution at the same interval (time points) as consumption of SCs.

The radioactive source of the densitoscanner is mounted in an aluminium frame to enable vertical movement. The tube was fastened with tapes to the frame to remain in a vertical position. The radioactive source used in this study is Cs-137 with a half-life of 30.17 years. This source constantly emits photons through the SCs towards the detector on the other side. The detector receives only these photons which were not absorbed by the sample in the SC. The scanning was repeated in both directions (up and downward) to obtain good resolution on the density distribution along the SCs. Since the results obtained with this measurement technique are relative, it is vital to calibrate the scanner. For this purpose, two tubes were added to the SC segment that were filled with saturated wet sand and the other one with water. These tubes were added at the bottom of the SC to measure their density together with the SC. As the density of both components is known, a calibration function can be calculated to scale the recorded data. The vertical resolution of density in this measurement is 0.5 cm with a sample rate of 3 Hz (3 samples per second). Figure 11 presents the setup of the radioactive Gammarray densitoscanner designed for this study.

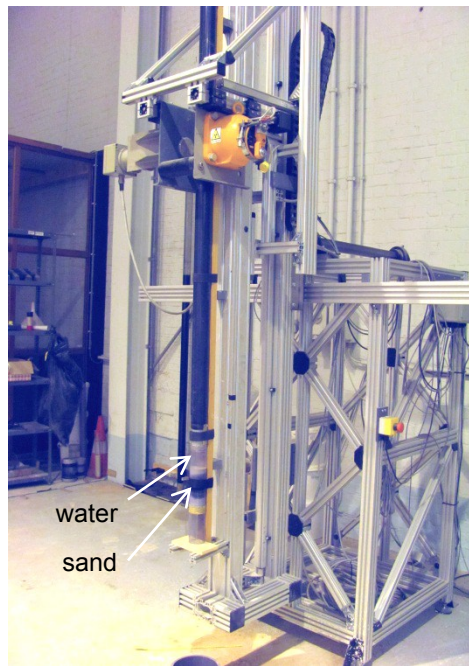


Figure 11 - The Radioactive densitoscanner and the installation setup for SCs

3.1.3. Grain size

The grain size distribution of the sub-samples from the SCs was measured by the Particle Size Analyser called Mastersizer 2000. Preceding the measurements, the sub-samples were exposed for a period of 60 s to ultrasonic displacement ($10 \mu\text{m}$) to disperse the big floc clusters as well as the air bubbles. Based on the grain size distribution, the Mastersizer calculates additional grain size characteristics of the sediment sample such as the average weighted surface and the average weighted volume. The device uses laser diffraction technology to measure the grain size characteristics. A sub-sample introduced in the machine is passed through a focused laser beam. The particles scatter the beams at an angle that is inversely proportional to their size. Bigger particles diffract light rays at smaller angles than fine particles. By scattering the light over 52 detectors under different angles, the Mastersizer provides grain size distribution of samples over a range between $0.02\mu\text{m}$ and $2000\mu\text{m}$. Particles larger than $2000\mu\text{m}$ are removed by sieving before introducing the sample into the Mastersizer. Figure 12 illustrates the Mastersizer 2000.



Figure 12 - Mastersizer 2000 from the laboratory of FHR.

3.1.4. Dry matter, organic and carbonate content

The dry matter, organic matter and carbonate content of the subsamples from SCs are measured using a Prepash 229 device (Figure 13). The ash weight of the subsamples is measured by an analytical balance during the heating trajectory. For this study, the Prepash measured the weight of the sample at 110°C, 550°C and 800°C. The water content of a mud sample is obtained by calculating the difference in sample weight between 110°C temperature and the initial weight. To obtain the organic matter content (*OC*), the same sample pre-dried at 110°C was heated up to 550°C. The difference in sample weight between 550°C and 110°C is the ignited organic matter called “loss on ignition” (*LOI*).

$$LOI_{550} = (Mass_{110} - Mass_{550})/Mass_{110} \times 100 \quad (1)$$

where LOI_{550} is the loss on ignition at 550°C, $Mass_{105}$ is the mass of sub-sample at 110°C and $Mass_{550}$ is the mass of sub-sample at 550°C. Using this value, the organic matter content (*OC*) can be derived from Equation (2) (Borovec, 1996).

$$OC = 0.092 + (0.465 \times LOI_{550}) \quad (2)$$

where *OC* is the organic content. Lastly, the carbonate content considered as loss on ignition for each sub-sample at 800°C, can be calculated using Equation (3).

$$LOI_{800} = (Mass_{550} - Mass_{800})/Mass_{110} \times 100 \quad (3)$$



Figure 13 - Prepash device from the laboratory of FHR to derive dry matter, organic matter and carbonate content.

3.2. Large consolidation column (LC)

The large consolidation columns (LCs) were mainly designed to enable monitoring of the consolidation behaviour of mud over a long period of time. To facilitate a systematic measurement, a setup was developed to measure continuously pore water pressures and mud interface of the LCs. In addition, at the end of the systematic measurement period, the consolidated mud within the large consolidation columns (LCs) was sub-sampled to analyse the rheological parameters, density, grains size and thermogravimetric parameters in the laboratory.

3.2.1. Measurement Frequency

Table 5 offers a summary of all the measurements conducted on the large consolidation columns (LCs) as well as the execution date of each measurement.

Table 5 - Dates and measurements conducted on LCs.

Date	07/4	08/4	09/4	10/4	14/4	18/8	19/8	20/8						
ZB														
DG														
RO														
IJ														
EM														
<p>Legend:</p> <table style="width: 100%; border: none;"> <tr> <td style="width: 50%; vertical-align: top;"> <div style="background-color: red; width: 20px; height: 10px; margin-bottom: 5px;"></div> Filling the LC </td> <td style="width: 50%; vertical-align: top;"> <div style="background-color: lightgreen; width: 20px; height: 10px; margin-bottom: 5px;"></div> DMA 38 </td> </tr> <tr> <td style="vertical-align: top;"> <div style="background-color: yellow; width: 20px; height: 10px; margin-bottom: 5px;"></div> Rheological parameters </td> <td style="vertical-align: top;"> <div style="background-color: cyan; width: 20px; height: 10px; margin-bottom: 5px;"></div> PrepAsh </td> </tr> <tr> <td></td> <td style="vertical-align: top;"> <div style="background-color: blue; width: 20px; height: 10px;"></div> Grain Size </td> </tr> </table>									<div style="background-color: red; width: 20px; height: 10px; margin-bottom: 5px;"></div> Filling the LC	<div style="background-color: lightgreen; width: 20px; height: 10px; margin-bottom: 5px;"></div> DMA 38	<div style="background-color: yellow; width: 20px; height: 10px; margin-bottom: 5px;"></div> Rheological parameters	<div style="background-color: cyan; width: 20px; height: 10px; margin-bottom: 5px;"></div> PrepAsh		<div style="background-color: blue; width: 20px; height: 10px;"></div> Grain Size
<div style="background-color: red; width: 20px; height: 10px; margin-bottom: 5px;"></div> Filling the LC	<div style="background-color: lightgreen; width: 20px; height: 10px; margin-bottom: 5px;"></div> DMA 38													
<div style="background-color: yellow; width: 20px; height: 10px; margin-bottom: 5px;"></div> Rheological parameters	<div style="background-color: cyan; width: 20px; height: 10px; margin-bottom: 5px;"></div> PrepAsh													
	<div style="background-color: blue; width: 20px; height: 10px;"></div> Grain Size													

3.2.2. Image Processing

The objective of the image processing is to measure the change in the water-sediment interface and pore water pressure over time. To track the pore water pressure over time, riser tubes were used that are connected to different heights on the large consolidation columns. By using image analysis methods, the water-sediment interface and the height of balls in the different riser tubes could be extracted from the time series of pictures which were taken at a rate of 1 image per 6 minutes. These two parameters are, amongst others, essential for describing the consolidation behaviour as these parameters give us the possibility to calculate the pore water overpressure and effective stresses. The time-lapse photography to assess the temporal behaviour of mud was started immediately after each large consolidation column was filled with its corresponding mud. Figure 14 illustrates the camera setup that is designed for this purpose. In total, 3 cameras continuously captured the evolution of the mud interface in 5 LCs (Large Consolidation Columns). The description on effective stresses is provided in section 3.2.3. A user guide to the image processing code is given in Cattrysse *et al.* (2015).

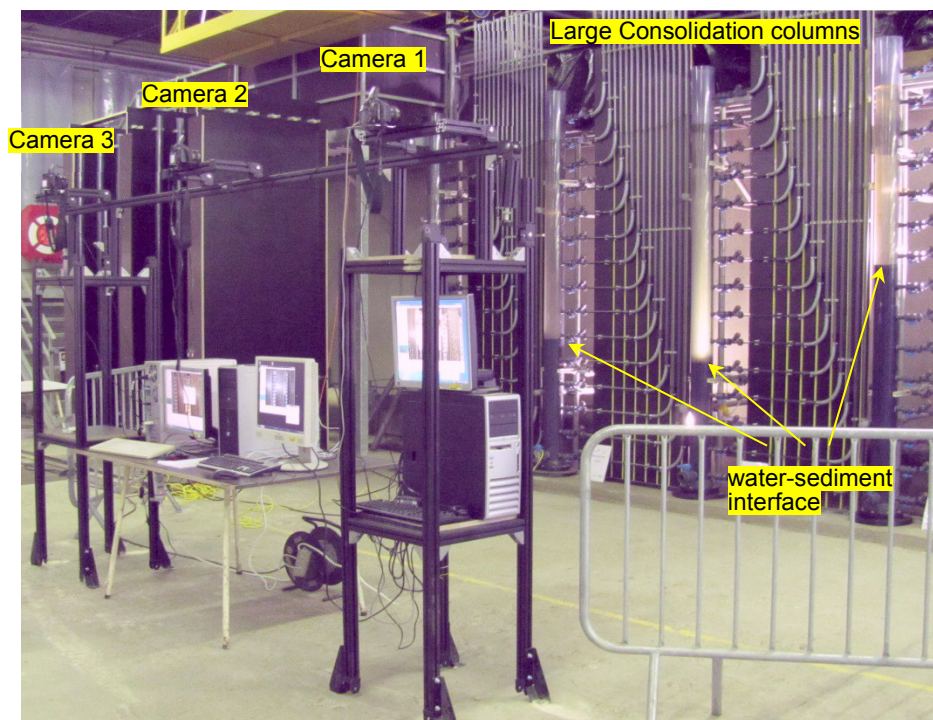


Figure 14 - The camera setup monitoring the evolution of mud consolidation within five LCs.

Calibration

The first step of the work flow is to construct a matrix that can convert the pixel distances to relative distances in meter. This was achieved by first finding the location of yellow rulers beside each riser tube, mounted on the black background. Due to bad focusing the resolution was insufficient to find the centimeter markings adequately. Instead, the decimeter markings (numbers indicating the decimeter) in red were used to get a pixel-to-distance map.

Figure 15 is a typical image taken by one of the camera's and illustrates the Rotterdam and Ijmuiden's LCs. The red circle in this figure highlights the location of floating balls in the riser tubes for Rotterdam's LC, used for the detection of pore water pressures. One can derive from the location of the floating balls in Figure 15 that the riser tubes at the left reveal the hydrostatic pressure because they are connected to the water layer above the mud. The riser tubes connected to the sediment column show a gradual increase in pore water pressure compared to the hydrostatic pressure. The blue circle in Figure 15 indicates the mud interface in this LC.

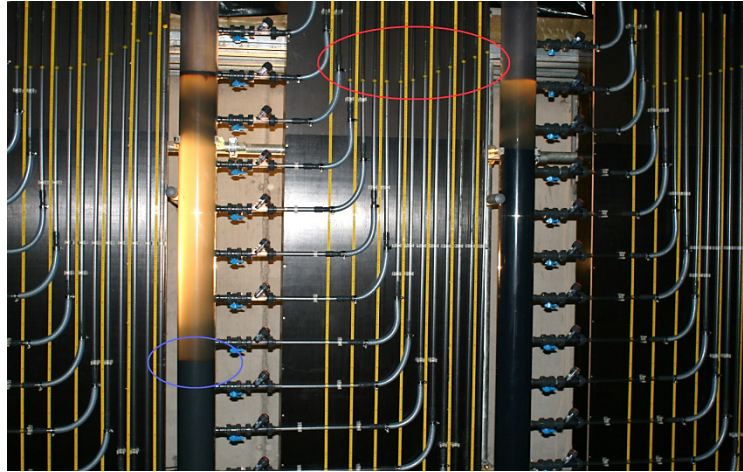


Figure 15 - Illustration of an image of one of the camera's with location of the yellow balls showing the pore water pressures for different riser tubes (red circle) and the mud interface (blue circle) in a LC.

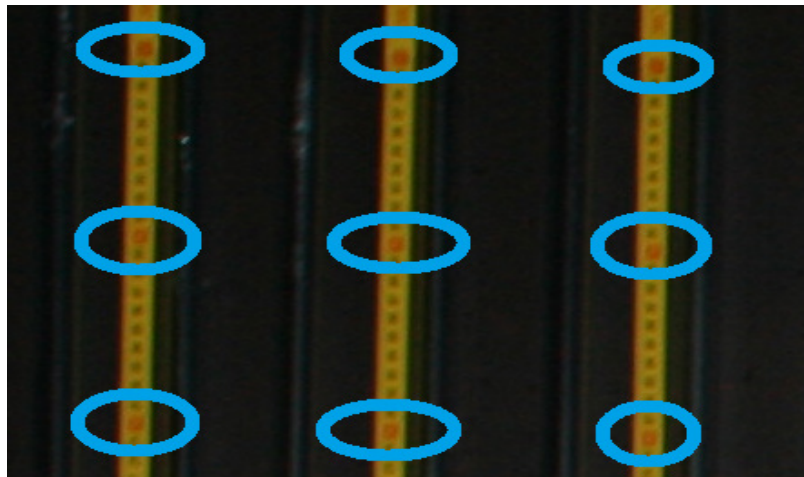


Figure 16 - Detecting the decimeter markings on yellow rulers.

Once the decimeter markings were detected (Figure 16), the decimeter markings that were equidistant (e.g. the 0.1m markings of the different rulers) were connected to each other using a 3rd degree polynomial (Figure 17).

These quasi horizontal 3rd degree polynomials span the complete x-axis. However, the fitted lines are based on the decimeter markings of a given harbour. In case of Figure 17, the fitted lines are based on the middle riser tubes, highlighted by a yellow box. By extrapolation, these lines are fit throughout the area outside of the yellow box. Since the 3rd degree polynomial function is prone to bending, this causes deviation of the lines at the sides of the images, which is not a problem since the region of interest to us (riser tubes) do not fall into the region where the function deviates significantly. Starting from this matrix, the relative location of each pixel of the image is estimated using intra and extrapolation methods. This generates a complete pixel-to-distance map (Figure 18). When the camera positions are changed (e.g. by accidental human interaction with the camera rig), a new pixel-to-distance map has to be generated.

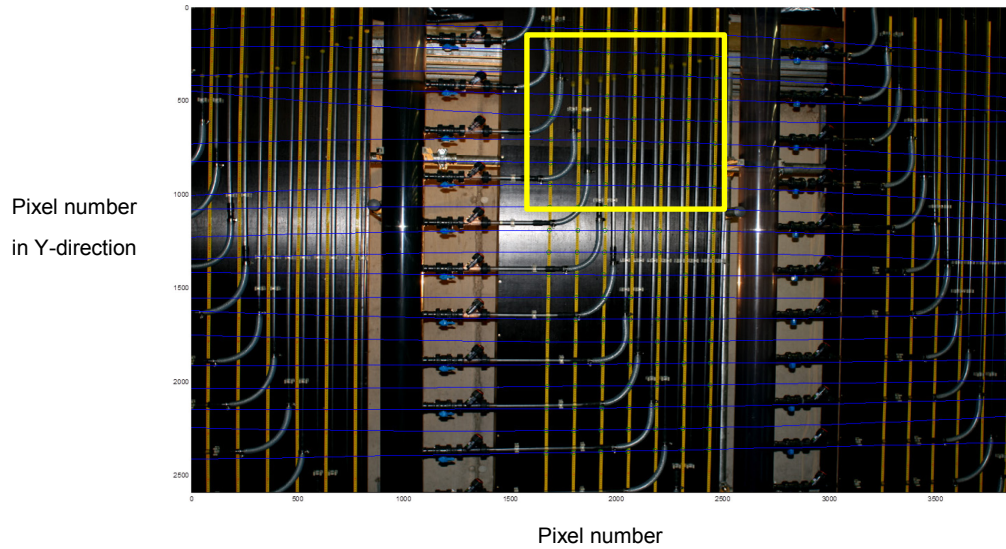


Figure 17 - The 3rd degree polynomial fit between the decimeter points on the rulers. The fitted lines are based on the area in the middle highlighted by a yellow box. Extrapolation causes bending of the lines at the sides of the image.

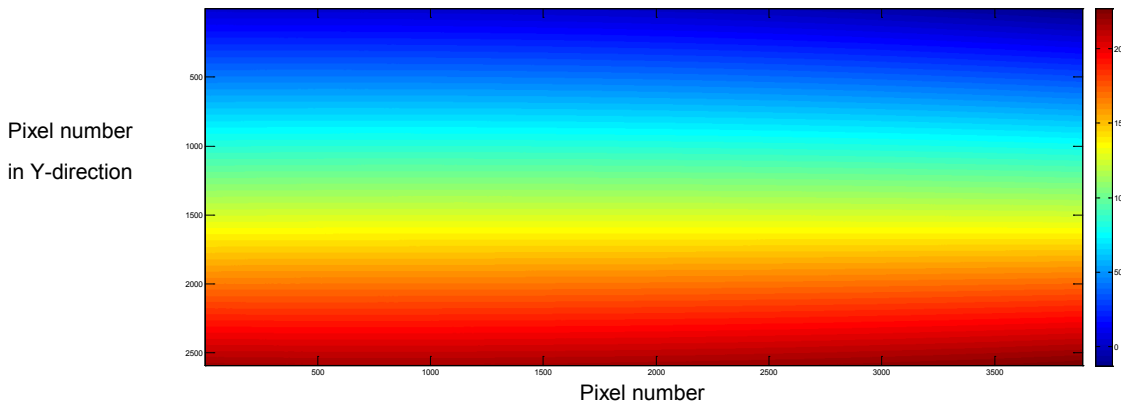


Figure 18 - A typical pixel-to-distance map.

Time series

To extract the position of the balls, the operator manually defines the riser tubes where the floating balls are expected to reside throughout the experiment. A certain band of pixels, which are expected to represent the location of the riser tubes (with balls somewhere in the tubes), is created and normalized in the X-direction. This results into 1 column of pixels for each riser tube. Within these columns of pixel intensities, the yellow spectrum is evaluated (Figure 19). Whereupon the column is added to a series of such columns throughout the time. The same procedure is used to detect the mud interface in LC. The difference for calculating the mud interface is that not the yellow spectrum is used for the time series, but the gradient in the Y direction of the complete spectrum as highlighted in white in Figure 20.

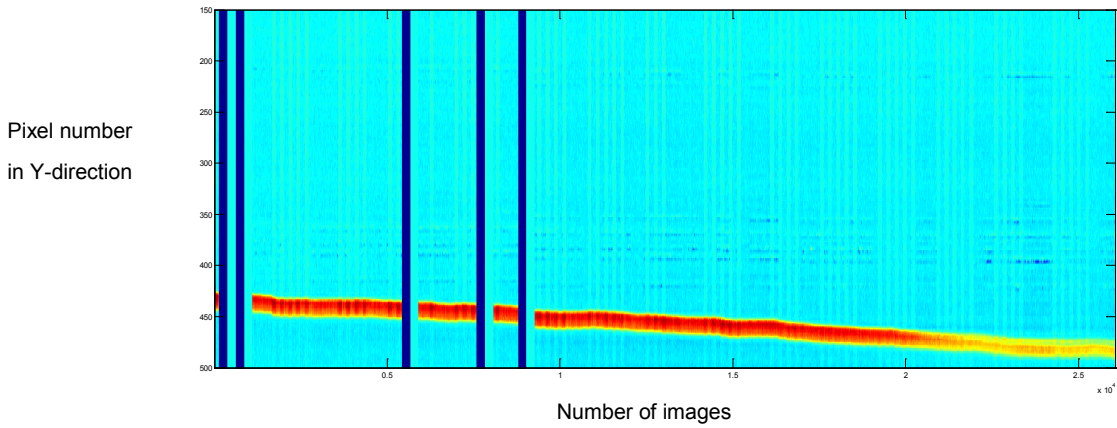


Figure 19 - Time series of the position of the ball in the riser tube of Zeebrugge LC over time by calculating the yellow spectrum of all pixels in a column.

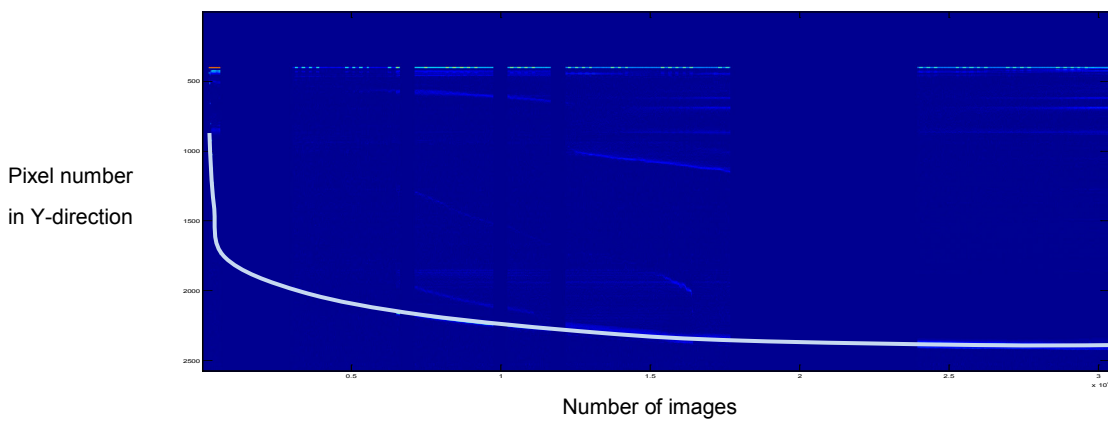


Figure 20 - Time series of the complete spectrum depicting the mud interface within one LC.

Extracting riser ball position

Knowing that the ball has an approximate width of 20mm, and each pixel represents 1mm distance in real life, a moving window of 1x20 pixels goes over each X value. The idea is that the highest array value per column (so per sample) of the generated matrix (Figure 19) is the center of the ball for that sample. To create useful charts, the pixel distance is then converted to an actual distance in meter using the pixel-to-distance map (Figure 21).

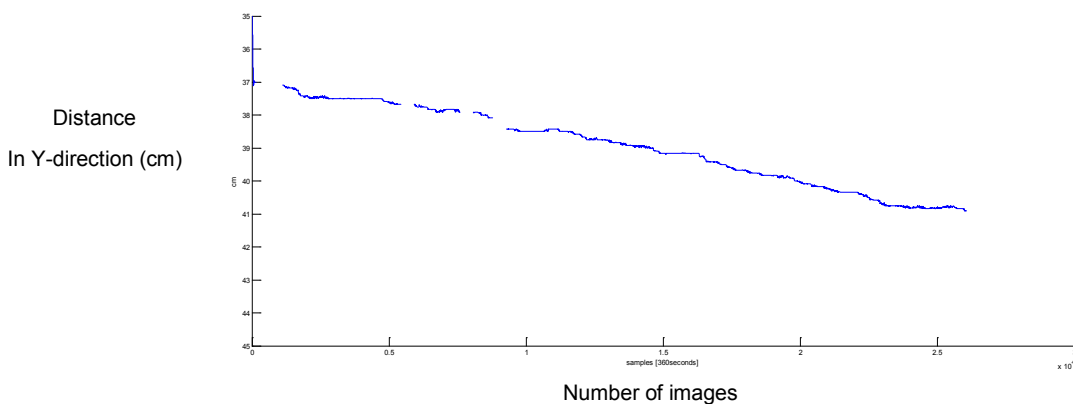


Figure 21 - The position of the ball in actual distance over time for one LC.

Extracting mud interface

To find the mud interface, the user gives an estimation of the interface in the time series of the consolidation column. Near to that estimation the maximum of the gradient time series is searched for each time step (each X-value) and used to generate a chart of the water sediment interface height in function of time (Figure 22).

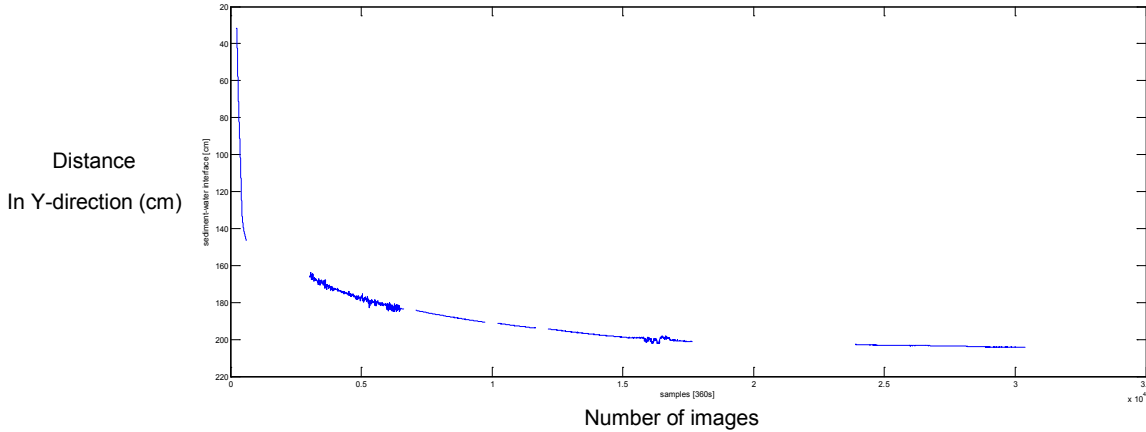


Figure 22 - The position of the mud interface in actual distance over time for Zeebrugge harbour.

Normalizing riser ball position

The goal of the image processing with respect to the riser tubes is ultimately to calculate the pore overpressure, which is the difference between pore water pressure and hydrostatic pressure, in the riser tubes. So it is necessary to know the water-air interface of each LC throughout time. Because of practical setup constraints, the water-air interface of a LC could not be extracted directly. The riser tube with filter closest to the LC (which connects at the highest point in the LC) was used to determine the hydrostatic pressure, because the level in this riser goes to hydrostatic pressure level in a matter of minutes to hours after initializing the test-setup. Once this initial time has elapsed, the riser tube closest to the LC can be used as normalizing factor to calculate the pore water pressure values from the other riser tubes.

3.2.3. Pore water pressure and effective stress

The height of a yellow ball (h) from the initiation of its corresponding riser tube gives an indication for the total pore water pressure that can be calculated by:

$$p = \rho_{sw}gh \quad (4)$$

where ρ_{sw} is the density of in situ water, g is the gravitational acceleration and h is the measured height in the risertube. Consolidation is the process whereby the load is gradually transferred from the fluid phase of the soil to the developing soil frame, thus while the consolidation proceeds the pore water over pressure decreases until consolidation stops when the value of pore water over pressure is negligible. By subtracting the hydrostatic pressure (p_h) from the total pore water pressure (p), the pore water over pressure (p_o) can be obtained by equation (5) (Merkelbach, 1998).

$$p_o = p - p_h \quad (5)$$

The values of pore water pressure over time can be used to calculate the effective stress. Effective stress is defined as the part of the normal stress supported by the solid particles, i.e. total stress minus pore water pressure (Berlamont et al., 1993). Total stress, σ , can be calculated by the integral of the mud density along the depth axis. With known values of pore water over pressure and total stress, the effective stress can be calculated as the difference of the total load and the pore water pressure (Merkelbach, 1998):

$$\sigma' = \sigma - p_o \quad (6)$$

4. References

- Berlamont, J., Van den Bosch, L. & Toorman, E. (1993). Effective stresses and permeability in consolidating mud, in: Edge, B.L. (Ed.) (1993). *Proceedings of the 23rd International Conference*, October 4-9, 1992, Venice, Italy. pp. 2962-2975.
- Borovec, Z. (1996). Evaluation of the concentrations of trace elements in stream sediments by factor and cluster analysis and the sequential extraction procedure. *Science of the Total Environment*, 177:237- 250.
- Buscall, R. (1990). The sedimentation of concentrated colloidal suspensions. *Colloids and surfaces* 43, 33–53.
- Cattrysse, H., Meshkati Shahmirzadi and Tomas Van Oyen (2015). Consolidation tests image processing software. UserGuide [MEMO]. Waterbouwkundig Laboratorium: Antwerpen. 5 p.
- Claeys, S., De Schutter, J., & Mostaert, F. (2009). Nautical Bottom Sediment Research. Comparison of in-situ rheological based instruments in the Sludge Test Tank. Antwerp: Flanders Hydraulic Research.
- Claeys, S.; Staelens P.; Van Hoestenbergh T.; Van Oyen T.; Verwaest T., D.; Mostaert, F. (2015a). Technical note: Technical scientific brainstorming to prepare the consolidation column project plan.. Flanders Hydraulics Research & Antea, Antwerp, Belgium.
- Claeys, S.; Staelens, P.; Heredia, M.; Vanlede, J.; Van Oyen, T.; Van Hoestenbergh T.; Toorman, E.; Verwaest, T.; Mostaert, F. (2015b). Sediment Related Nautical Research: Rheological Measurement Protocol for cohesive sediment. Version 3.0. WL Rapports, 13_117. Flanders Hydraulics Research & Antea Group, DOTocean and KULeuven: Antwerp, Belgium. In preparation.
- Delefortrie, G., Vantorre, M. & Eloit, K. (2005). Modelling navigation in muddy areas through captive model tests. *J. Mar. Sci. Technol.*, 10:188–202.
- Eijkelkamp (2005). Operating instructions: 04.23 sediment core sampler, type Beeker [MANUAL]. Available on: https://www.eijkelkamp.com/download.php?file=M10423e_Becker_sampler_a426.pdf [date of consultation: 03/04/2015]
- Fontein, W; Wal, J. (2006). Assessing nautical depth efficiently: in terms of rheological characteristics, in: (2006). Evolutions in hydrography, 6th - 9th November 2006, Provincial House Antwerp, Belgium: Proceedings of the 15th International Congress of the International Federation of Hydrographic Societies. Special Publication (Hydrographic Society), 55: pp. 149-152.
- Guiarte, R.C., Kelly, W.E. & Nacci, V.A. (1979). Rheological methods for predicting cohesive erosion. In: *Proc. 15th Annual Conf. of the Marine Technology Soc.*, New Orleans, LA, pp. 251-258.
- Huysentruyt, H. and Berlamont, J. (1993). 'Consolidation'. Section 4.1 in: On the methodology and accuracy of measuring physico-chemical properties to characterize cohesive sediments. *Report of the MAST-1 G6-M, Cohesive Sediment Project Group* (ed. J.C. Winterwerp), pp.65-78, Commission of the European Communities, Directorate General XII.
- Johansen, C. (1998). Dynamics of Cohesive Sediments. Aalborg: Aalborg Universitetsforlag. (Series Paper; No.16).
- Kerckaert, P., Malherbe B. and Bastin A. (1985). Navigation in muddy areas: the Zeebrugge experience. PIANC Bulletin No. 48.
- Kerckaert P., Vandenbossche D., Malherbe B., Druyts M., Van Craenenbroeck K. (1988). Maintenance dredging at the port of Zeebrugge: Procedures to achieve an operational determination of the nautical bottom. 9th KVV Harbour Congress, Antwerp, pp. 4.13-32.
- Lee, B.J., Fettweis, M., Toorman, E., Moltz, F. (2012). Multimodality of a particle size distribution of cohesive suspended particulate matters in a coastal zone. *J. Geophysical Research*, 117, C03014, 17pp.
- Lintern D. G. (2003). Influences of flocculation on bed properties for fine-grained cohesive sediment Doctor of Philosophy, St Catherine's College, University of Oxford, Hilary Term.
- Merckelbach L.M. (1999). Consolidation and strength evolution of Dollard mud Measurement. Report on laboratory experiments no. 4-99. *The Netherlands Technology Foundation (STW) and the Commission of the European Communities, DeurganckdokXII, MAST3-COSINUS Project* .

- Merckelbach L.M. (1998). Consolidation and strength evolution of Caland-Beer Channel mud. Measurement report on laboratory experiments no. 7-98. *The Netherlands Technology Foundation (STW) and the Commission of the European Communities*, DeurganckdokXII, MAST3-COSINUS Project.
- Michaels, A. S. and Bolger, J. C. (1962). Settling rates and sediment volumes of flocculated kaoline suspensions. *Industrial and Engineering Chemistry, Fundamentals* 1: 24-33.
- Mieghem, Jo., Smits, J. and Sas, M. (1997). Large-scale Dewatering of Fine-grained Dredged Material. *Terra et Aqua* – No. 68 :21-28.
- Migniot, C. (1987). Synthèse des connaissances sur le tassement et la rhéologie des vases. Laboratoire Central d'Hydraulique de France Sept. rap. 54238: 89 pages.
- PIANC (1997) Approach channels – A guide for design, Final report of the joint Working Group PIANC and IAPH, in cooperation with IMPA and IALA. Supplement to PIANC Bulletin, No. 95, 108 pp.
- Staelens P., Geirnaert K., Deprez S., Noordijk A., & Van Hassent, A. (2013). Monitoring the consolidation process of mud from different European ports in a full scale test facility. Conference Proceedings, WODCON XX: The Art of Dredging, Brussels, Belgium.
- Toorman, E.A. (1997). Modelling the thixotropic behaviour of dense cohesive sediment suspensions. *Rheologica Acta*, Vol.36(No.1):56-65.
- U. S. Army Corps of Engineers. (1987). Confined Disposal of Dredged Material, 1987, *Engineer Manual* No. 1110-2-5027. Washington, D. C. 20314-1000.
- Van Craenenbroeck, K. & Vantorre, M. (1991). Navigation in muddy areas: establishing the navigable depth in the port of Zeebrugge. *Proceedings of the CEDA-PIANC Conference (incorporating CEDA Dredging Days)*, 13-14 November 1991, Amsterdam. pp. 1-16.
- Van Craenenbroeck, K. & Vantorre, M. (1992). Navigation in muddy areas: establishing the navigable depth in the port of Zeebrugge. *Terra et Aqua*. 47: 3-12.
- Van Goethem, J. and Berlamont, J. (1985). Avoiding mud accumulation in harbours and their entrances. *Interim Research Report to S.B.B.M- SixCo*, Hydraulics Laboratory: 52 pages (in Dutch).
- Wurpts R. & Greiser N. (2008). Monitoring and dredging technology in muddy layers. *Chinese-German Joint Symposium on Hydraulic and Ocean Engineering*, August 24-30, 2008, Darmstadt. pp. 385-392.
- Wurpts, R. and Torn, P. (2005). 15 Years experience with fluid mud: definition of the nautical bottom with rheological parameters. *Terra et Aqua*, 99, 22–32.
- Huang, Z., and Huhe, A. (2009). A laboratory study of rheological properties of mudflows in Hangzhou Bay, China, *International Journal of Sediment Research*. Vol. 24, pp.409-423.

5. Appendix

Abbreviations

IBC	Bulk container
SC	Small consolidation column
LC	Large consolidation column
ZB	Harbor of Zeebrugge
DG	Deurganckdok
RO	Harbor of Rotterdam
IJ	Harbor of IJmuiden
EM	Harbor of Emden
EFC	Equilibrium flow curves
<i>OC</i>	Organic matter content
<i>LOI</i>	Loss on ignition
FHR	Flanders Hydraulics Research

Terminologies

Consolidation	Controlled by permeability and effective stress. When the water is pushed out from the bulk mud. This generally happens if the bounds between particles (floc clusters) increases.
Sodium adsorption ratio	The concentrations of solids dissolved in the water.
Cation exchange capacity	The total capacity of a soil to hold exchangeable cations
Specific surface	The ratio of the total surface of a substance (such as an adsorbent) to its volume
Humus	The organic component of soil, formed by the decomposition of leaves and other plant material by soil microorganisms.
Beaker sampler	An acrylic sampling tube used to capture completely undisturbed samples
Gelling point	The transition between sedimentation and consolidation
Rheology	The branch of physics that deals with the deformation and flow of matter, especially the non-Newtonian flow of liquids and the plastic flow of solids.
Peak shear stress	The maximum resistance of undisturbed mud against an external deformation rate
Equilibrium shear stress	When the rate of growth and break down of the bounds are equal in a sample exposed to a given deformation rate
Effective stress	A force that keeps a collection of particles rigid.
Pore water over pressure	By subtracting the hydrostatic pressure from the total pore pressure, the pore water over pressure is obtained



Waterbouwkundig Laboratorium

Flanders Hydraulics Research

Berchemlei 115

B-2140 Antwerp

Tel. +32 (0)3 224 60 35

Fax +32 (0)3 224 60 36

E-mail: waterbouwkundiglabo@vlaanderen.be

www.waterbouwkundiglaboratorium.be